GENERIC HYPERBOLIC KNOT COMPLEMENTS WITHOUT HIDDEN SYMMETRIES

JASON DEBLOIS AND PRIYADIP MONDAL

ABSTRACT. We describe conditions under which, for a two-component hyperbolic link in S^3 with an unknotted component, one can show that all but finitely many hyperbolic knots obtained by $1/n$-surgery on that component lack hidden symmetries. We apply these conditions to the two-component links through nine crossings in the Rolfsen table, and to various other links in the literature. In each case we show that having no hidden symmetries is "generic" among knots produced in this way.

It is well known to those in the know that a "generic" hyperbolic knot complement in S^3 has no hidden symmetries. This is directly asserted, for instance, in [23, §5.3], and it is supported by abundant computational evidence: only three are known with hidden symmetries, and the roughly 330,000 knots with at most fifteen crossings and hyperbolic complements supply no additional examples. Indeed, it has been conjectured that no hyperbolic knot complement in S^3 has hidden symmetries, beyond the three already known [2, Conjecture 1.1].

The data above is collected by exploiting the following fundamental characterization due to Neumann–Reid [17, Proposition 9.1]: a hyperbolic knot complement in S^3 has a hidden symmetry if and only if it covers an orbifold with a *rigid cusp*: one with a rigid Euclidean orbifold (a triangle orbifold or its orientation-preserving double cover) as a horospherical cross-section. This implies for instance that a hyperbolic knot complement with hidden symmetries has cusp field $\mathbb{Q}(i)$ or $\mathbb{Q}(i\sqrt{3})$, a condition which is straightforward to check computationally using SnapPy [6] and Sage [7] (or Snap, see [5]) and rules out the vast majority of knots in the tables.

However this condition is typically not easy to rule out for all members, or even the generic member, of an infinite family of hyperbolic knot complements. Among such families, only those of the two-bridge knots other than the figure-eight [23], the $(-2, 3, n)$-pretzel knots [13], and certain highly twisted pretzel knots with at least five twist regions [15, Prop. 7.5] have been shown not to have hidden symmetries, to the best of our knowledge of the literature. (We also note related significant work due to Hoffman [9], Boileau–Boyer–Cebanu–Walsh [2], and Millichap–Worden [16].)

This paper expands the above collection. Along the way we provide a tool for proving that the generic member of certain infinite families of hyperbolic knot complements lacks hidden symmetries, in many cases by a SnapPy/Sage computation analogous to the one mentioned above. Our main computational result is:

Theorem 2.3. *Let $L = K \sqcup K'$ be a hyperbolic two-component link in S^3 with 9 or fewer crossings, such that K' is unknotted. With the standard framing on K', the complement of the knot K_n obtained from L by $1/n$ surgery on K' has no hidden symmetries for all but finitely many $n \in \mathbb{Z}$.*

Following standard practice, above we say a knot or link is *hyperbolic* if its complement admits a complete, finite-volume hyperbolic structure. And the "standard framing" refers in this case to meridian-longitude coordinates on the boundary of a small regular neighborhood $\mathcal{N}$ of K' such that the meridian bounds a disk in $\mathcal{N}$ that intersects K' once, and the longitude lies in the disk that K' bounds. For such K' and any $n \in \mathbb{Z}$, it is a standard fact that K_n is a knot in S^3 (see eg. [24, Ch. 9.H]), and the hyperbolic Dehn surgery theorem [26, Th. 5.8.2] (cf. eg. [19], [20]) implies that K_n is hyperbolic for all but finitely many n.

There are 90 two-component links with up to 9 crossings in Rolfsen's table [24, Appendix C], of which 82 are hyperbolic. Each of these has at least one unknotted component, and many yield knots K_n that are not two-bridge or $(-2, 3, n)$-pretzels, so here we are exhibiting many new infinite families of knot complements whose generic members lack hidden symmetries.

Our results rest on the almost trivial observation Lemma 1.1, which asserts that there can be only finitely many cusp shapes among any family of one-cusped manifolds with bounded volume that all cover orbifolds with rigid cusps. One way in which this can occur is due to *geometric isolation*, a phenomenon studied extensively by Neumann–Reid [18], where the shape of one cusp of a fixed manifold is independent of the shapes of the others. Example 1.4 draws on the proof of Theorem 2 of [18], which exhibits instances of geometric isolation, to describe an infinite family of one-cusped manifolds with bounded volume and a fixed cusp shape.

Combining Lemma 1.1 with basic material on hyperbolic Dehn surgery yields our main technical result, Theorem 1.2. Below we record its consequence obtained by specializing to the setting of two-component links with an unknotted component and applying [17, Prop. 9.1]. Here the *shape* of a cusp of a complete hyperbolic 3-manifold is the Euclidean similarity class of a horospherical cross-section.

Corollary 1.3. *Let $L = K \sqcup K'$ be a hyperbolic two-component link in S^3 such that K' is unknotted. With the standard framing on K', if infinitely many of the knots K_n obtained by $1/n$ surgery on K' have hidden symmetries, then:*

(1) *The shape of the cusp c of $S^3 - L$ corresponding to K covers a rigid Euclidean orbifold; and*
(2) *c is geometrically isolated from the other cusp of $S^3 - L$.*

Above, *geometric isolation* is a property defined in [18] in which the complete structure on one cusp of a (say, two-cusped) hyperbolic manifold does not change under any Dehn filling of the other cusp. Conclusion (2) above is stronger than its correspondent in Theorem 1.2 thanks to an observation of D. Calegari from §1.2 of his study of geometric isolation [3], that the parameter of one cusp of a two-cusped hyperbolic 3-manifold depends holomorphically on the surgery parameter of the other (cf. our proof of Cor. 1.3).

In Section 2 we apply Corollary 1.3 to prove Theorem 2.3. Of the Corollary's two criteria, (1) is straightforward to automate. We have done just that, writing a short script that iterates over SnapPy's table of two-component links, outputting the cusp information of each and using Sage to identify the cusp fields. This shows that all but five of the 82 hyperbolic two-component links up to 9 crossings do not give rise to infinitely many hyperbolic knots whose complements have hidden symmetries, see Lemma 2.2.

The complements of the remaining five fall into two isometry classes: that of the Whitehead link 5_1^2, and that of 6_2^2. For each of these link complements, its cusp covers a rigid Euclidean orbifold, and we obtain the conclusion by appealing to Corollary 1.3(2). (The knots produced by $1/n$ surgery on a component of the Whitehead link are twist knots and hence are also covered by the results of [23].) Non-geometric isolation of the Whitehead link complement's cusps follows from Theorem 6.1 of [17], and in Section 3 we follow the approach of that paper to prove non-geometric isolation of the cusps of 6^2_2.

The results of this paper suggest the following form of "genericity" for hyperbolic knot complements without hidden symmetries.

Conjecture 0.1. For any $R > 0$, at most finitely hyperbolic knot complements in S^3 have hidden symmetries and volume less than R.

Of course this is significantly weaker than Conjecture 1.1 of [2], but it should also be more approachable using current technology.

1. Rigid cusps and complex moduli

The **cusp shape** of a given cusp of a complete, non-compact hyperbolic 3-manifold or 3-orbifold is the Euclidean similarity class of a horospherical cusp cross-section. The cusp is **rigid** if and only if the cusp shape is the quotient of $\mathbb{R}^2$ by a Euclidean triangle group (of type $(2,4,4)$, $(3,3,3)$, or $(2,3,6)$) or its index-two orientation-preserving subgroup. The name reflects the fact that the Euclidean structures on these orbifolds, and only these among all Euclidean 2-orbifolds, admit no deformations through Euclidean structures.

Lemma 1.1. *Suppose for some $B > 0$ that $\{M_j\}$ is a collection of complete, one-cusped hyperbolic 3-manifolds, each with volume at most B, such that for every j there is an orbifold cover $M_j \to O_j$ to an orbifold with a rigid cusp. Then among all M_j there are only finitely many cusp shapes.*

Proof. For each j the branched cover $M_j \to O_j$ restricts on any horospherical cusp cross-section of M_j to a branched cover of a horospherical cusp cross-section of O_j. It follows that the lattice in $\mathbb{R}^2$ that uniformizes the cusp shape of M_j is a subgroup of the uniformizing lattice for the cusp shape of O_j, so of the $(2,3,3)$, $(2,4,4)$, or $(2,3,6)$-triangle group. The index of this subgroup is either the degree d_j of $M_j \to O_j$ or $2d_j$, depending on whether the cusp cross-section of O_j is a triangle orbifold or turnover.

Let V be the minimal volume of complete hyperbolic 3-orbifolds [14]. Then

$$d_j \leq \frac{B}{V}$$

The lemma now follows from the basic fact that any finitely generated group, so in particular each of the $(2,3,6)$-, $(2,4,4)$-, and $(3,3,3)$-triangle groups, has only finitely many subgroups of bounded index. □

In Example 1.4 we will exhibit an infinite family of one-cusped hyperbolic manifolds with a fixed cusp shape, each member of which covers an orbifold with a rigid cusp. They are obtained by hyperbolic Dehn filling one cusp of a two-cusped manifold constructed in the proof of Theorem 2 of [18]. The other cusp of this manifold is geometrically isolated from the first, a property that follows from the fact that the manifold covers an orbifold with a rigid cusp. We have deferred describing the example until the end of this section because writing down the details takes some space, and we prefer to proceed now to the main results.

Suppose $T = \mathbb{C}/\Lambda$ is an oriented Euclidean torus, where $\Lambda \subset \mathbb{C}$ is a lattice, and fix an oriented pair of generators μ, λ for Λ. This is equivalent to choosing the oriented pair $[\mu], [\lambda]$ of generators for $H_1(T)$, sometimes called a "meridian-longitude" pair. The **complex modulus** of T is the ratio λ/μ in the upper half-plane $\mathbb{H}^2$. Changing the choice of generating pair changes the complex modulus by the action of a Möbius transformation, and it is not hard to see that its $\mathrm{PSL}_2(\mathbb{Z})$-orbit is a complete similarity invariant of T.

Suppose that M is a complete, oriented hyperbolic 3-manifold with finite volume and k cusps $c_1, \ldots c_k$. A horospherical cross section of c_i is a Euclidean torus, and for a fixed choice of generators $[\mu_i], [\lambda_i]$ for its first homology we call the complex modulus of this cross section the **cusp parameter** of c_i. (Here $[\mu_i], [\lambda_i]$ is oriented with respect to the boundary orientation the cross section of c_i inherits from the compact core of M.) The $\mathrm{PSL}_2(\mathbb{Z})$-orbit of the cusp parameter of c_i is thus a complete invariant of its cusp shape.

Now suppose N is a complete hyperbolic 3-manifold obtained by Dehn filling some cusps of M. If c_i is not filled then $[\mu_i]$ and $[\lambda_i]$ determine generators for the corresponding cusp of N, and therefore also a particular choice of cusp parameter. The relationship between the cusp parameters of M and N, as laid out by Thurston [26] and further clarified by Neumann–Zagier [19], is key to the result below.

Theorem 1.2. *Suppose that $\{M_j\}_{j=1}^{\infty}$ is a collection of distinct complete, one-cusped hyperbolic 3-manifolds, each obtained by Dehn filling all cusps but a fixed one, c, of a complete, oriented hyperbolic 3-manifold N of finite volume. If M_j branched covers an orbifold with a rigid cusp for each j then:*

(1) *the cusp shape T of c covers a rigid Euclidean orbifold; and*
(2) *M_j has cusp shape T for all but finitely many j.*

Moreover, if $[\mu], [\lambda]$ is an oriented basis for $H_1(c)$, and $[\mu_j], [\lambda_j]$ is the corresponding basis for H_1 of the cusp of M_j, then $\lambda_j/\mu_j = \lambda/\mu$ for all but finitely many j.

Proof. Suppose M has k cusps, enumerated $c_1, \ldots, c_k$ so that $c = c_1$. The key fact is that $\lambda/\mu = \tau_1(\mathbf{0})$, and $\lambda_j/\mu_j = \tau_1(\mathbf{u}_j)$ for all but finitely many j, where $\tau_1(\mathbf{u})$ is a holomorphic function on a neighborhood U of $\mathbf{0} \in \mathbb{C}^k$, and $\{\mathbf{u}_j\} \subset U$ converges to $\mathbf{0}$ as $j \to \infty$. Here we are using the notation from Section 4 of Neumann–Zagier [19], where this is described in detail. Briefly, for any hyperbolic structure (not necessarily complete) on M, we take $\mathbf{u} = (u_1, \ldots, u_k)$ where for $1 \leq i \leq k$, u_i records the *complex length* of μ_i. This is the logarithm of the derivative of its holonomy in the affine structure that a cross section of c inherits from M, which is also the log of the ratio of the eigenvalues of its holonomy in $\mathrm{PSL}(2, \mathbb{C})$. The branch of log is chosen so that $u_i = 0$ at the complete structure on M. It is proved in [19] that $\mathbf{u}$ holomorphically parametrizes the deformation variety of M near the point corresponding to this structure.

For $\mathbf{u}$ such that $u_i \neq 0$ — that is, for which c_i is not a complete cusp — $\tau_i(\mathbf{u})$ is defined as v_i/u_i, where v_i is the logarithm of the derivative of the holonomy of λ_i. By Lemma 4.1 of [19], taking $\tau_i(\mathbf{u}) = \lambda_i/\mu_i$ when $u_i = 0$ extends it to an analytic function of $\mathbf{u}$. Since $\tau_1(\mathbf{u})$ is in particular continuous on U it follows that $\tau_1(\mathbf{u}_j) \to \tau_1(\mathbf{0})$ in $\mathbb{H}^2$ as $j \to \infty$; hence the same is true of the orbits of these points in $\mathbb{H}^2/\mathrm{PSL}_2(\mathbb{Z})$. Work of Thurston (cf. [19, Theorem 1A]) implies that M_j has volume less than M for all j, so Lemma 1.1 now implies that all but finitely many of these orbits must equal that of $\tau_1(\mathbf{0})$. Since these orbits are discrete subsets of $\mathbb{H}^2$ it follows that $\tau_1(\mathbf{u}_j) = \tau_1(\mathbf{0})$ for all but finitely many j, and the result is proved. □

Corollary 1.3. *Let $L = K \sqcup K'$ be a hyperbolic two-component link in S^3 such that K' is unknotted. With the standard framing on K', if infinitely many of the knots K_n obtained by $1/n$ surgery on K' have hidden symmetries, then:*

(1) *The shape of the cusp c of $S^3 - L$ corresponding to K covers a rigid Euclidean orbifold; and*
(2) *c is geometrically isolated from the other cusp of $S^3 - L$.*

Proof. For a hyperbolic link $L = K \sqcup K'$ with K' unknotted, and any $n \in \mathbb{Z}$, it follows from [24, Ch. 9.H] (as mentioned before) that $1/n$ Dehn filling on the cusp c' of $S^3 - L$ corresponding to K' yields a knot complement $S^3 - K_n$. By the hyperbolic Dehn surgery theorem, this knot complement is hyperbolic for all but finitely many n. For each n such that $S^3 - K_n$ has hidden symmetries, it covers an orbifold with a rigid cusp by Prop. 9.1 of [17]. Condition (1) of the Corollary therefore follows immediately from the corresponding condition of Theorem 1.2.

The Corollary's condition (2) follows from the Theorem's, together with an observation from Section 1.2 of [3]. Taking u and u' to be the respective complex lengths of the meridians of c and c', we note that the complete hyperbolic structure on each $S^3 - K_n$ obtained from $S^3 - L$ by hyperbolic Dehn filling corresponds to a point with $u = 0$, since c is complete. The restriction of τ_1 (as described in the proof of Theorem 1.2) to the $u = 0$ locus is an analytic function of the single variable u'. Its values are constant on the infinite sequence corresponding to $S^3 - K_n$, so it is constant. As observed in [3], this implies geometric isolation. □

Remark. To the results in this section that use analyticity of the cusp parameter we should perhaps add a hypothesis that the manifolds in question admit a genuine ideal triangulation by positively oriented tetrahedra. The results of [19] seem to require this, which is unknown for arbitrary finite-volume hyperbolic 3-manifolds.

Petronio–Porti proved the hyperbolic Dehn filling theorem in general using a broader class of "triangulations" [20], but they explicitly did not attempt to establish in the general context that the complete structure is a smooth point of the deformation variety. See the thorough discussion in the Introduction to [20]. As mentioned there, there is a cohomology-based approach to proving the hyperbolic Dehn surgery theorem that does establish smoothness of the representation variety near the complete structure (see eg. [12]). But we do not know how to prove analyticity of the cusp parameter using this approach.

In any case, for us this is a theoretical rather than practical objection, since the manifolds we work with in the following sections are explicitly triangulated.

Example 1.4. The proof of Theorem 2 of [18] describes a finite-volume, two-cusped hyperbolic 3-manifold $\mathbb{H}^3/G_4$ that covers an orbifold $\mathbb{H}^3/G_1$ with one pillowcase and one $(2,4,4)$-turnover cusp. Here a *pillowcase cusp* has a cross section which is a sphere with four cone points, each with cone angle π; that is, the cross section is the double of a Euclidean rectangle. A $(2,4,4)$-*turnover cusp* has a cross-section that is the double of an isosceles right triangle.

The map $\mathbb{H}^3/G_4 \to \mathbb{H}^3/G_1$ factors as a sequence of double orbifold covers $\mathbb{H}^3/G_i \to \mathbb{H}^3/G_{i-1}$ for $i = 2, 3, 4$. Let c_1 be the pillowcase cusp of $\mathbb{H}^3/G_1$, and for $i > 1$ let c_i be the cusp of $\mathbb{H}^3/G_i$ that covers c_{i-1}. (Note that c_i is unique for each i since $\mathbb{H}^3/G_4$ has only two cusps.) By construction, c_1 and c_2 are pillowcase cusps, whereas c_3 and c_4 are torus cusps and the cover $c_4 \to c_3$ is not branched.

We claim that there exist infinitely many orbifold Dehn fillings of the pillowcase cusp c_1 of $\mathbb{H}^3/G_1$ such that for each one there is a corresponding filling of the cusp c_i of $\mathbb{H}^3/G_i$, $i = 2, 3, 4$, and an extension of the orbifold cover $\mathbb{H}^3/G_i \to \mathbb{H}^3/G_{i-1}$ over the Dehn fillings. Let us assume this claim for the moment.

All but finitely many fillings of c_4 yield one-cusped hyperbolic manifolds, so this is true of the given fillings as well. For each hyperbolic filling of c_4, Mostow rigidity implies that the covering transformation of the Dehn filled $\mathbb{H}^3/G_4$ corresponding to the Dehn filled $\mathbb{H}^3/G_3$ is realized by an isometry, and it follows that the Dehn filled $\mathbb{H}^3/G_3$ is a one-cusped hyperbolic orbifold. Similarly, for hyperbolic fillings on c_4 the corresponding fillings of $\mathbb{H}^3/G_2$ and $\mathbb{H}^3/G_1$ are hyperbolic.

For each hyperbolic filling on c_1 the shape of the cusp of the filled $\mathbb{H}^3/G_1$ stays the same: it is the unique Euclidean $(2, 4, 4)$ turnover up to similarity. Therefore each corresponding filling of $\mathbb{H}^3/G_4$ covers an orbifold with a rigid cusp. These fillings also all have the same cusp shape, since their cusps correspond to a fixed cover of the cusp of $\mathbb{H}^3/G_1$.

In proving the claim we will first review pillowcases, their covers, and their fillings. We wish to advertise at the beginning that a necessary criterion for the existence of fillings of $\mathbb{H}^3/G_4$ covering those of $\mathbb{H}^3/G_1$ will emerge from the discussion below — that is, there is actually something to check holds in this particular sequence of covers.

Every Euclidean pillowcase is isomorphic to the quotient of $\mathbb{R}^2$ by the group H generated by order-two rotations a, around $(0, 1)$, b, around $(0, 0)$, and c, around $(1, 0)$. This group preserves the integer lattice, with fundamental domain $[0, 1] \times [-1, 1]$ and presentation

$$H = \langle\, a, b, c \,|\, a^2 = b^2 = c^2 = (abc)^2 = 1 \,\rangle.$$

Its final conjugacy class of elliptics is represented by abc, which fixes $(1, 1)$.

The unique torsion-free index-two subgroup K of H is the kernel of the map to $\mathbb{Z}/2\mathbb{Z} = \{0, 1\}$ sending each generator, and hence also abc, to 1. It is the lattice generated by $x = cb$ and $y = ab$, which respectively act on $\mathbb{R}^2$ by translation in the x- and y-directions. For each $p, q \in \mathbb{Q} \cup \{\infty\}$ (taking (p, q) to be $(1, 0)$, $(0, 1)$, or a pair of relatively prime integers with $q > 0$), the lines of slope p/q project to a foliation of $\mathbb{R}^2/K$ by primitive closed geodesics corresponding to $x^p y^q \in K$. For each line of slope p/q that does not intersect the integer lattice, its projection to $\mathbb{R}^2/K$ maps homeomorphically under the further projection to $\mathbb{R}^2/H$.

The model for orbifold Dehn filling of the pillowcase is the inclusion of $\mathbb{R}^2/H$ to the "pillow", a trivial two-string tangle in the ball where the cone angle is π around each string. The pillow can be modeled as the quotient of the infinite cylinder $\mathbb{D}^2 \times \mathbb{R}$ by rotations of order two around the x-axis and its translate through $(0, 0, 1)$. Its orbifold fundamental group is infinite dihedral. If one tangle string joins the cone points of $\mathbb{R}^2/H$ corresponding to b and c, and the other those corresponding to a and abc, then the inclusion-induced map on H sets $b = c$ and $a = abc$. Its kernel is $\langle x \rangle$ (which is normal since each of a, b and c conjugates x to $x^{-1} = bc$).

Now for the orbifold $\mathbb{H}^3/G_1$, having identified a horospherical cross-section of c_1 with $\mathbb{R}^2/H$, we define the orbifold Dehn filling along $p/q \in \mathbb{Q} \cup \{\infty\}$ by truncating c_1 along the cross section and gluing on a pillow via an orbifold isomorphism from

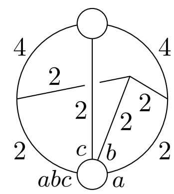

FIGURE 1. $\mathbb{H}^3/G_1$ with labeled pillowcase cusp.

its boundary to the cross section that takes x to $x^p y^q$. For $r, s \in \mathbb{Z}$ such that $ps - qr = 1$, such an isomorphism is induced by $\gamma = \left(\begin{smallmatrix} p & r \\ q & s \end{smallmatrix}\right) \in \mathrm{SL}(2,\mathbb{Z})$. (It is not hard to show that $\mathrm{SL}(2,\mathbb{Z})$ normalizes H.)

The isomorphism determined by γ preserves the cone point of $\mathbb{R}^2/H$ corresponding to b, and it takes the cone point corresponding to c to one corresponding to the element of H fixing (p,q). We note that each point of the integer lattice is K-equivalent to exactly one of $(0,0)$, $(1,0)$, $(0,1)$ or $(1,1)$. This is determined by the parities of its entries since elements of K translate by even integers in each variable. It follows that $\gamma c \gamma^{-1} = a$ if p is even and q is odd, it is c if p is odd and q is even, and it is abc if both are odd.

We may identify the cross section of c_1 with $\mathbb{R}^2/H$ in such a way that c_2 corresponds to the kernel H_2 of the map to $\mathbb{Z}/2\mathbb{Z} = \{0,1\}$ sending a to 1 and b and c to 0. Then for $p/q \in \mathbb{Q} \cup \{\infty\}$, there is an orbifold cover of the p/q-Dehn filling of c_1 by a corresponding Dehn filling of c_2 if and only if the map above induces one from the dihedral group $H/\langle x^p y^q \rangle$ onto $\mathbb{Z}/2\mathbb{Z}$. Since the image of b is equal to that of $\gamma c \gamma^{-1}$ in $H/\langle x^p y^q \rangle$, we must have $\gamma c \gamma^{-1}$ conjugate to c for this to occur. That is, we require p odd and q even.

H_2 is generated by b, c, and aba, with its fourth conjugacy class of elliptics represented by $ababc = (abc)c(abc)$. Its unique torsion-free index-two subgroup H_3 is therefore generated by x and $y^2 = (aba)b$. This therefore corresponds to the torus cusp c_3 of $\mathbb{H}^3/G_3$ covering c_2. For any slope λ on a cross-section of c_3, the orbifold cover from c_3 to c_2 automatically extends to an orbifold cover from the Dehn filling of c_3 to the Dehn filling of c_2 along λ, where the solid torus covers the pillow corresponding to the index-two cyclic subgroup of the infinite dihedral group.

For p and q as above we may write $x^p y^q$ as $x^p (y^2)^{q/2}$, so the lift to c_3 of the surgery slope on c_1 has coordinates p and $q/2$ in the generators x and y^2 for H_3. The cover of c_3 by c_4 corresponds to a map $H_3 \twoheadrightarrow \mathbb{Z}/2\mathbb{Z}$, and there is a corresponding cover of the filling along $x^p y^q$ if and only if this slope is contained in the kernel. Recalling that p is required to be odd and there is no stipulation on the parity of $q/2$, what must be avoided is the case that x is sent to 1 and y^2 to 0. For in this case the filling slope would map non-trivially to $\mathbb{Z}/2\mathbb{Z}$ regardless of the parity of q. If both x and y^2 are sent to 1 then choosing q such that $q/2$ is odd yields a covering filling, and if x is sent to 0 then we must choose q congruent to 0 modulo 4.

We will show that the sequence of covers $\mathbb{H}^3/G_i \to \mathbb{H}^3/G_{i-1}$ described in [18] prescribes that x is sent to 0, given our choice of identification of H with the orbifold fundamental group of c_1. This identification is pictured in Figure 1, where we have duplicated the left half of Figure 6 of [18] and added labels on the tangle strings intersecting the pillowcase cusp of $\mathbb{H}^3/G_1$. The element x of H is represented by a simple closed curve on the pillowcase separating the tangle string endpoints labeled b and c from those labeled a and abc.

It is straightforward to check using [18, Fig. 6] that the cover $c_2 \to c_1$ corresponds to the kernel of the map to $\mathbb{Z}/2\mathbb{Z}$ sending a to 1 and b and c to 0. That is, it unwraps the cone points of the pillowcase labeled a and abc, and each of those labeled b and c has two preimages in c_2. The lift of x to the pillowcase cross section of c_2 separates the two preimage points of b and those of c. From Figure 7 of [18] we therefore find that its lift to the torus cross section of c_3 is vertical, transverse to the annulus fiber described at the top of p. 230. As described there, the cover $\mathbb{H}^3/G_4$ is fibered over S^1 with twice-punctured torus fiber, and its cover $\mathbb{H}^3/G_3$ is two-to-one on each fiber and one-to-one in the transverse direction. So its restriction to c_4 corresponds to the kernel of the map $H_3 \to \mathbb{Z}/2\mathbb{Z}$ that sends x to 0 and y^2 to 1. This proves the claim.

2. Data on two-component links

In this section we prove our main computational result Theorem 2.3, on knots in S^3 obtained by surgery on one component of a two-component link with up to nine crossings. Our main tool is a computation using SnapPy [6] and Sage [7], based on the following well known fact:

Fact 2.1. *If the shape of a cusp c of a complete, finite-volume hyperbolic 3-manifold covers a rigid Euclidean orbifold then the parameter of c lies in $\mathbb{Q}(i)$ or $\mathbb{Q}(\sqrt{-3})$.*

This follows from the fact that the Euclidean lattice uniformizing a horospherical cross section of such a cusp c lies in a $(2,4,4)$-, $(3,3,3)$-, or $(2,3,6)$-triangle group. The following sequence of commands call SnapPy from within Sage to check the field generated by each cusp of the complement of each hyperbolic two-component link with at most nine crossings.

```
sage:  import snappy
sage:  for M in snappy.LinkExteriors(num_cusps=2)[:90]:
....:    if M.volume() > 1:
....:      L = M.cusp_translations()
....:      z = L[0][0]/L[0][1]
....:      w = L[1][0]/L[1][1]
....:      print (M,factor(z.algdep(10)),factor(w.algdep(10)))
....:
```

Reading the above from the top, the first line calls SnapPy from within Sage. (This is assuming that the two programs have been configured to work with each other, see the SnapPy website for instructions on how to accomplish this.) The second line iterates over a pre-built table of triangulated complements of links up to 10 crossings in SnapPy; we have restricted to two-component links through 9 crossings. The next line excludes the non-hyperbolic examples, which SnapPy computes to have 0 or infinitesimal volume. (These are 4^2_1, 6^2_1, 7^2_7, 8^2_1, 9^2_{43}, 9^2_{49}, 9^2_{53} and 9^2_{61}. It is not hard to show directly that each is non-hyperbolic.)

The command "`M.cusp_translations()`" produces a list of ordered pairs of complex numbers, each giving a set of generators for a Euclidean lattice uniformizing an embedded cross section of a cusp of M. In our setting, since M is a two-component link complement there are two pairs. The next two lines compute shapes

z and w of the two cusps of M by dividing the first entry of each pair by the second. We finally print the notation from [24, App. C] for the link corresponding to M, together with factored polynomials satisfied by each of z and w. In particular, the command "`z.algdep(`n`)`" finds a polynomial of degree at most n that is (approximately) satisfied by the (approximate) algebraic number z.

Out of the 82 hyperbolic two-component links tested, only 5_1^2, 6_2^2, 7_8^2, 8_{15}^2, and 9_{47}^2 have cusp parameters which lie in either $\mathbb{Q}(i)$ or $\mathbb{Q}(\sqrt{-3})$. Applying criterion (1) of Corollary 1.3 therefore yields:

Lemma 2.2. *Let $L = K \sqcup K'$ be a hyperbolic two-component link in S^3 with at most nine crossings that is not one of 5_1^2, 6_2^2, 7_8^2, 8_{15}^2, or 9_{47}^2, such that K' is unknotted. With the standard framing on K', the complement of the knot K_n obtained from L by $1/n$ surgery on K' has no hidden symmetries for all but finitely many $n \in \mathbb{Z}$.*

In fact the complements of 7_8^2, 8_{15}^2, and 9_{47}^2 are each isometric to that of the Whitehead link 5_1^2. This can be verified with SnapPy, and it is also possible to show directly: the unknotted component of 7_8^2 bounds a disk which intersects its other component, a trefoil knot, twice. Cutting along the three-punctured sphere that is this disk's intersection with the link complement, twisting by a multiple of 2π, and regluing yields a sequence of isometries between link components. Twisting by 2π in one direction reverses one crossing of the trefoil component of 7_8^2, which thus unknots yielding 5_1^2. Twisting by 2π in the other direction yields 9_{47}^2. On the other hand, 8_{15}^2 is easily seen to be obtained from 5_1^2 by a similar operation.

The complement of 6_2^2 is commensurable with the Bianchi group $\mathrm{PSL}(2, \mathcal{O}_3)$ and that of 5_1^2 (and hence also of 7_8^2, 8_{15}^2, and 9_{47}^2) is commensurable with $\mathrm{PSL}(2, \mathcal{O}_1)$. Here $\mathcal{O}_d$ is the ring of integers of $\mathbb{Q}(\sqrt{-d})$. These each fail the second criterion of Corollary 1.3, which we use to prove our result.

Theorem 2.3. *Let $L = K \sqcup K'$ be a hyperbolic two-component link in S^3 with 9 or fewer crossings, such that K' is unknotted. With the standard framing on K', the complement of the knot K_n obtained from L by $1/n$ surgery on K' has no hidden symmetries for all but finitely many $n \in \mathbb{Z}$.*

Proof. Following Lemma 2.2 and the remarks below it, it remains only to consider the complement of the Whitehead link 5_1^2 and that of 6_2^2. We will show in each case that neither cusp is geometrically isolated from the other. In each case the link has a symmetry that exchanges its two components; this is clear from the picture of 6_2^2 in [24, App. C], and it is clear from Thurston's picture of the Whitehead link in [26, §3.3]. Thus in each case it is sufficient to fix one cusp of the link complement and show it is not geometrically isolated from the other. But this was already shown for 5_1^2 by Theorem 6.1 of [17].

We perform the analogous computation for 6_2^2 in the next section, proving in Proposition 3.2 that its cusps are not geometrically isolated from each other. $\square$

3. The link 6_2^2

In this section, we study the complement of 6_2^2 (see picture in [24]) in S^3. Our main result is Proposition 3.2, which shows that the parameter of one of its cusps is non-constant near its complete hyperbolic structure.

The correspondence between two bridge links and words in R and L's is explained by Futer in appendix of [8] and by Millichap and Worden in [16]. It is noted in

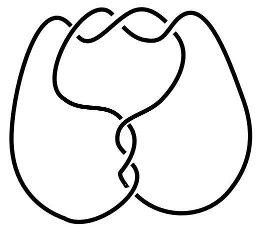

FIGURE 2. 6_2^2 is a two bridge link

([16]) that the link 6_2^2 and its mirror image correspond to the words L^2R^2 and R^2L^2 respectively. They also argue in [16] that the complement of the mirror image of 6_2^2 in S^3 and complement of 6_2^2 in S^3 are isometric. Keeping this in mind, from now on we will abuse the notation 6_2^2 to mean the mirror image of 6_2^2. Figure 2 represents two bridge link structure of 6_2^2 showing how it corresponds to the word R^2L^2.

To understand the tetrahedral decomposition of $S^3 \setminus 6_2^2$, first we briefly discuss the tetrahedral decomposition of a two bridge link given by Sakuma and Weeks in [25]. Refer to section II.2 of [25] (see also section 3 of [16] and A.2 of [8]) for a complete and rigorous description. They ([25]) first consider triangles with vertices labelled by the continued fractions corresponding to the two bridge links given by the "subwords from the left" of the word determining the original two bridge link. They explain how one obtains triangulations of $\mathbb{R}^2$ (denoted as $\widetilde{\Delta}_i$ in their paper) induced by these triangles. For each $i \in \{2, \dots, c-3\}$ where $c = \mathit{length}(\text{Two bridge link word}) + 2$, they consider a pair of ideal tetrahedra formed in between the restriction of the triangulations $\widetilde{\Delta}_i$ and $\widetilde{\Delta}_{i+1}$ in the fundamental domain of "π rotation action" on $\mathbb{R}^2 \setminus \mathbb{Z}^2$ with the faces of these tetrahedra being the triangles in those triangulations. Two faces coming from $\widetilde{\Delta}_i$'s $i \neq 2, c-1$ are paired if those trace back to the same triangle in a triangulation. For $\widetilde{\Delta}_2$ and $\widetilde{\Delta}_{c-1}$, they pair two adjacent triangles along the edge of slope $\frac{1}{2}$ and the continued fraction of the subword which excludes the last two letters respectively by the linear maps which switches the distinct vertices and identifies the same vertices. Finally they prove in Theorem II.2.4 of [25] that these ideal tetrahedra and the face pairings determine a tetrahedral decomposition of the two bridge link complement in S^3.

We use Sakuma and Weeks' tetrahedral decomposition for two bridge link complements (theorem II.2.4 in [25]) to see the tetrahedral decomposition of $S^3 \setminus 6_2^2$ in figure 3. Pairs of consecutive triangulations $\mathbb{R}^2$ are shown in the left of figure 3 (cf. figure II.2.5 in [25], figure 3 in [16]). We straighten up these pairs in the right of figure 3 to see three pairs of ideal tetrahedra $(\mathbb{T}_i, \mathbb{T}_i')$, $i \in \{2, 3, 4\}$. We denote the faces of tetrahedra by F_i and $\widetilde{F}_j$, for $i \in \{1, \dots, 8\}$ and $j \in \{1, 2, 3, 4\}$. We use [25]'s face pairing to see that F_i is identified with F_i' for $i \in \{1, \dots, 8\}$ and $\widetilde{F}_j$ is identified with $\widetilde{F}'_j$ for $j \in \{1,2,3,4\}$ by the linear maps given as follows:

$$
\begin{array}{lcr}
F_1: & ((1,0),(4,1),(3,1)) \leftrightarrow ((1,0),(4,1),(3,1)) & :F'_1 \\
F_2: & ((0,0),(3,1),(1,0)) \leftrightarrow ((0,0),(3,1),(1,0)) & :F'_2 \\
F_3: & ((0,0),(3,1),(2,1)) \leftrightarrow ((2,0),(5,1),(4,1)) & :F'_3 \\
F_4: & ((1,0),(4,1),(2,0)) \leftrightarrow ((1,0),(4,1),(2,0)) & :F'_4 \\
F_5: & ((0,0),(4,1),(3,1)) \leftrightarrow ((0,0),(4,1),(3,1)) & :F'_5 \\
F_6: & ((0,0),(4,1),(1,0)) \leftrightarrow ((6,2),(10,3),(7,2)) & :F'_6 \\
F_7: & ((1,0),(5,1),(4,1)) \leftrightarrow ((7,2),(3,1),(4,1)) & :F'_7 \\
F_8: & ((1,0),(5,1),(2,0)) \leftrightarrow ((3,1),(6,2),(7,2)) & :F'_8 \\
\widetilde{F}_1: & ((0,0),(2,1),(1,0)) \leftrightarrow ((2,0),(4,1),(3,1)) & :\widetilde{F}'_1 \\
\widetilde{F}_2: & ((1,0),(3,1),(2,1)) \leftrightarrow ((1,0),(3,1),(2,0)) & :\widetilde{F}'_2 \\
\widetilde{F}_3: & ((0,0),(3,1),(7,2)) \leftrightarrow ((10,3),(3,1),(7,2)) & :\widetilde{F}'_3 \\
\widetilde{F}_4: & ((0,0),(7,2),(4,1)) \leftrightarrow ((6,2),(3,1),(10,3)) & :\widetilde{F}'_4
\end{array}
$$

From [26] (see also [19], [22]), we know that the set of *edge invariants* $\{w_1, w_2, w_3\}$ of an ideal tetrahedra satisfies :

$$w_1 w_2 w_3 = 1, \quad w_1 = \frac{1}{(1-w_2)}, \quad w_3 = 1 - \frac{1}{w_2} \tag{1}$$

We denote the set of edge invariants of $\mathbb{T}_2$, $\mathbb{T}'_2$, $\mathbb{T}_3$, $\mathbb{T}'_3$, $\mathbb{T}_4$ and $\mathbb{T}'_4$ by $\{x_1, x_2, x_3\}$, $\{x'_1, x'_2, x'_3\}$, $\{y_1, y_2, x_3\}$, $\{y'_1, y'_2, y'_3\}$, $\{z_1, z_2, z_3\}$ and $\{z'_1, z'_2, z'_3\}$ respectively. We see from the face paring in figure 3 that the edge equations of this decomposition are:

$$x_2 x'_1 y_1 z_2 y'_1 x_1 x'_2 x_1 y_1 z'_2 y'_1 x'_1 = 1 \tag{2}$$
$$x_3 x'_3 y_2 = 1 \tag{3}$$
$$x_3 x'_3 y'_2 = 1 \tag{4}$$
$$y_2 z'_1 z_1 = 1 \tag{5}$$
$$y'_2 z'_1 z_1 = 1 \tag{6}$$
$$z_2 z'_3 y'_3 x_2 y_3 z_3 z'_2 z_3 y'_3 x'_2 y_3 z'_3 = 1 \tag{7}$$

Equation (3) and (4) imply $y_2 = y'_2$. So, $y_1 = y'_1$ and $y_3 = y'_3$.
Then (4) and (5) gives $z_1 z'_1 = x_3 x'_3$ implying $\frac{1}{(1-z_2)(1-z'_2)} = \frac{(x_2-1)(x'_2-1)}{x_2 x'_2}$. So, we get:

$$x_2 x'_2 = (x_2 - 1)(x'_2 - 1)(1 - z_2)(1 - z'_2)$$

Equation (2) gives us

$$1 = x_2 x'_2 z_2 z'_2 (x_1 x'_1)^2 (y_1 y'_1)^2 = x_2 x'_2 z_2 z'_2 (x_1 x'_1)^2 y_1^4 = \frac{x_2 x'_2 z_2 z'_2}{(1-x_2)^2 (1-x'_2)^2 (1-y_2)^4}$$

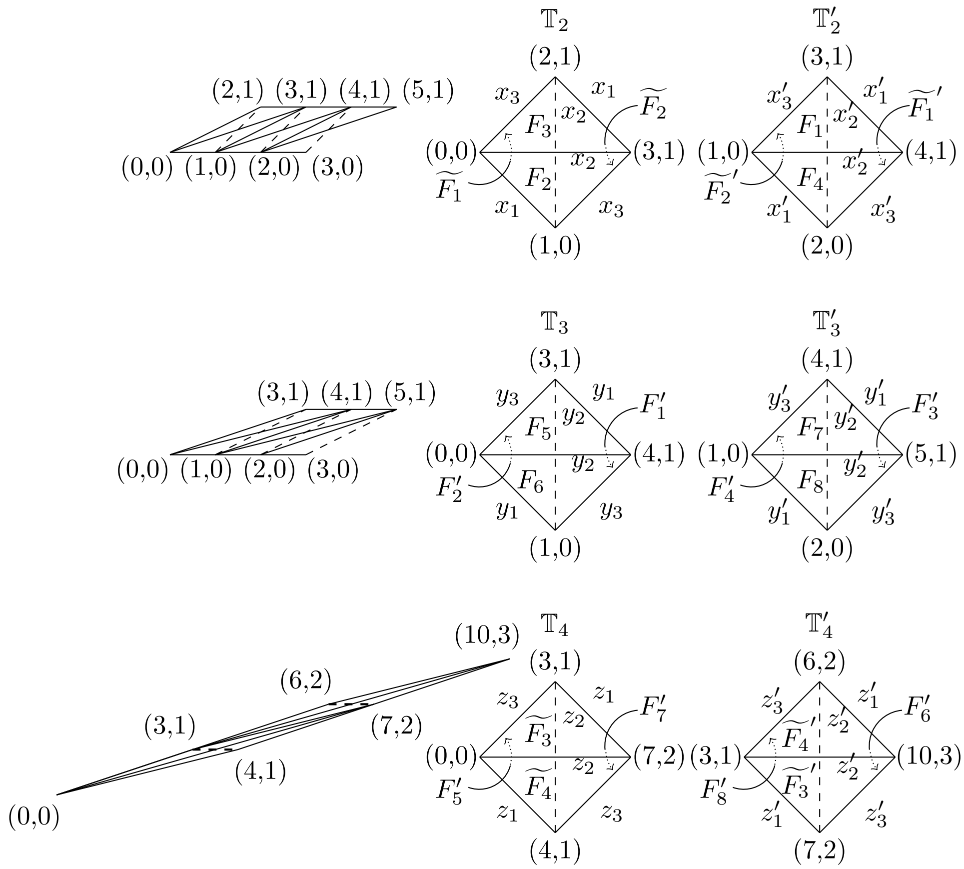

FIGURE 3. Tetrahedral Decomposition of $S^3 \setminus 6_2^2$

$$
\begin{aligned}
\text{Now,} \quad z_2 z_3' y_3' x_2 y_3 z_3 z_2' z_3 y_3' x_2' y_3 z_3' &= z_2 z_2' x_2 x_2' (z_3 z_3')^2 (y_3 y_3')^2 \\
&= z_2 z_2' x_2 x_2' \frac{(z_2-1)^2 (z_2'-1)^2 (y_2-1)^4}{z_2^2 z_2'^2 y_2^4} \\
&= \frac{x_2 x_2'}{z_2 z_2'} \frac{(1-y_2)^4}{(1-z_2)^2(1-z_2')^2} \\
&= 1.
\end{aligned}
$$

This implies that equation (7) can be derived from equation (2).

So the hyperbolic structures on the 6_2^2 link complement in S^3 correspond bijectively to four-tuples $(x_2, x_2', z_2, z_2') \in (\mathbb{C}^+)^4$ satisfying the equations below (where $\mathbb{C}^+ = \{z = x + iy \in \mathbb{C} \mid y > 0\}$):

$$x_2 x_2' = (x_2 - 1)(x_2' - 1)(1 - z_2)(1 - z_2') \tag{8}$$

$$z_2 z_2' (1 - z_2)^2 (1 - z_2')^2 = x_2 x_2' (1 - y_2)^4 = x_2 x_2' (z_2 + z_2' - z_2 z_2')^4 \tag{9}$$

Definition 3.1. The *deformation variety* of the 6_2^2-link complement is the set V of $(x_2, x_2', z_2, z_2') \in \mathbb{C}^4$ satisfying equations (8) and (9).

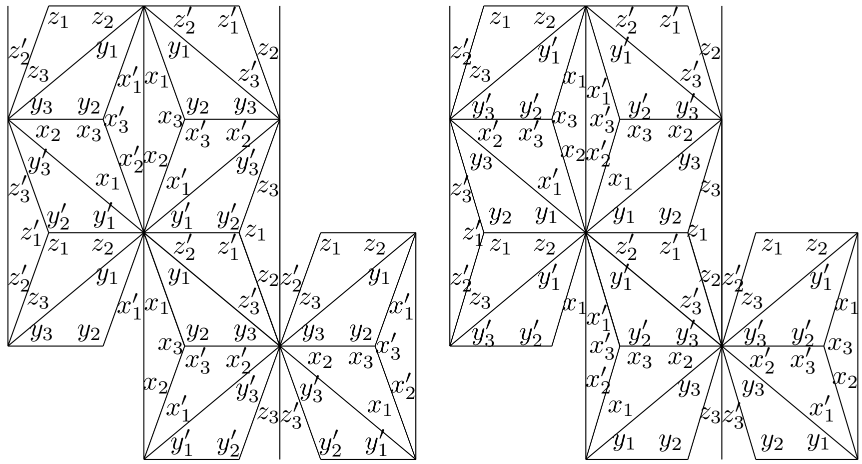

FIGURE 4. Cusp triangulation at $[(0,0)]$ (Left) and $[(1,0)]$(Right)

In section II.4, [25] shows how to find the "cusp triangulation" for a two bridge link complement in its "canonical decomposition" into ideal tetrahedra given by Theorem II.2.4 of [25]. We mimic the cusp triangulation picture of a two bridge link complement (figure II.4.1 of [25]) in figure 4 to represent the cusp triangulation pictures at [(0,0)] and [(1,0)]. Let $\{m_1,\ l_1\}$ and $\{m_2,\ l_2\}$ be the meridian-longitude pair of the fundamental groups of the links at the cusps [(0,0)] and [(1,0)] respectively. We denote the derivative of the holonomy of an element γ of the fundamental group of a link by $H'(\gamma)$. Then by the description given in section 2 of [19] and figure 4, we get:

$$H'(m_1) = -y_1'x_1'x_2x_1y_1z_2' \tag{10}$$

$$H'(l_1) = z_2y_1x_1'x_1y_1y_3x_2'y_3'z_3z_3'y_3'y_1' \tag{11}$$

$$H'(m_2) = -z_2y_1'x_1x_2x_1'y_1 \tag{12}$$

$$H'(l_2) = z_2y_1'x_1x_1'y_1'y_3'x_2y_3z_3z_3'y_3y_1 \tag{13}$$

Neumann and Reid([17]) showed that the cusp parameter at a complete cusp of Whitehead link complement can be expressed as a function of one edge invariant. We follow their technique to write our cusp parameter at a complete cusp as a function of x_2 and x_2'. We assume that the cusp at [(0,0)] is complete. From figure

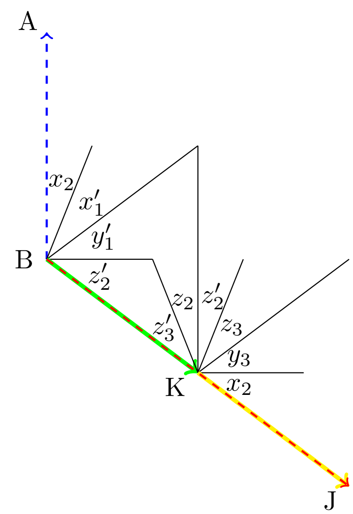

Figure 5. Longitude-Meridian Pair and Cusp Parameter

5 (cf. figure 14 and figure 15 in [17]), we see that

$$\begin{aligned}
\tau &= \frac{\vec{BJ}}{\vec{BA}} \\
&= \frac{\vec{BK}}{\vec{BA}} + \frac{\vec{KJ}}{\vec{BA}} \\
&= \frac{1}{(x_2 x'_1 y'_1 z'_2)} - \frac{1}{(x_2 x'_1 y'_1 z'_2 z'_3 z_2 z'_2 z_3 y_3 x_2)} \\
&= \frac{1}{(x_2 x'_1 y'_1 z'_2)} \left(1 - \frac{z'_1 z_1}{y_3 x_2}\right) \\
&= \frac{(1 - y'_2)}{x_2 x'_1 z'_2} \left(1 - \frac{x_3 x'_3}{y_3 x_2}\right) \\
&= \frac{(1 - \frac{1}{x_3 x'_3})}{x'_2 x'_1 \left(1 - \frac{1}{z_1}\right)} \left(1 - \frac{x_3 x'_3}{x_2 (1 - x_3 x'_3)}\right) \\
&= \frac{x_1 (x_3 x'_3 + x'_2 (x_3 x'_3 - 1)^2)(x_2 (1 - x_3 x'_3) - x_3 x'_3)}{(x_3 x'_3 + x'_2 (x_3 x'_3 - 1)^2 - 1)}
\end{aligned}$$

We use [10] to simply this to

$$\tau = \frac{1}{x_2} \left(\frac{1}{(x_2 - 1)} + \frac{x_2^3}{(x_2 - 1)(x'_2 - 1)} + \frac{(1 + x_2)}{x'_2} - \frac{x_2^2}{(x_2 + x'_2 - 1)} \right) \tag{14}$$

Proposition 3.2. *The parameter τ of the cusp of the 6_2^2 link complement at $[(0,0)]$ is not constant near the complete structure on the subvariety of the deformation variety V (see Definition 3.1) where this cusp is complete.*

Before proving the proposition we record a lemma.

Lemma 3.3. *For any hyperbolic structure on the 6_2^2 link complement with a complete cusp at $[(0,0)]$, we have $x_2 z'_2 = x'_2 z_2$.*

Proof. Since the cusp at [(0,0)] is complete, from (10) we have, $H'(m_1) = y_1^2 x_1 x_1' x_2 z_2' = -1$. This implies $(x_2 z_2')(x_1 x_1') = -(1-y_2)^2$. So, equation (9) yields

$$\begin{aligned}\frac{x_2 x_2'}{z_2 z_2'} \frac{(x_2 z_2')^2 (x_1 x_1')^2}{(1-z_2)^2(1-z_2')^2} &= z_3 z_3' (x_2 z_2')^2 (x_1 x_1')(z_1 z_1')^2 \\ &= \frac{x_1 x_1' x_3 x_3' (x_2 z_2')^2}{z_2 z_2'} = \frac{(x_2 z_2')^2}{x_2 x_2' z_2 z_2'} = 1\end{aligned}$$

This shows that $x_2 z_2' = x_2' z_2$. □

Proof. It is possible to use equations (8) and (9) to write z_2 and z_2' as functions of x_2 and x_2', so these give coordinates for the deformation variety V. The equation of Lemma 3.3 thus can be rewritten in terms only of x_2 and x_2', and by the Lemma, it cuts out the subvariety of V where the cusp at $[(0,0)]$ is complete. We will take x_2 as a parameter for this subvariety, and treat x_2' as a function of x_2. It will emerge from computations that we perform below, and the implicit function theorem, that this is possible near the complete structure. For now, we take it for granted.

Taking a derivative in (14) now yields:

$$\begin{aligned}\frac{d\tau}{dx_2} = \frac{1}{x_2}[&-\frac{1}{(x_2-1)^2} + \frac{3x_2^2}{(x_2-1)(x_2'-1)} - \frac{x_2^3}{(x_2'-1)(x_2-1)^2} \\ &- \frac{bx_2^3}{(x_2-1)(x_2'-1)^2} + \frac{1}{x_2'} - \frac{(1+x_2)b}{{x_2'}^2} - \frac{2x_2}{x_2+x_2'-1} + \frac{x_2^2(1+b)}{(x_2+x_2'-1)^2}] \\ &- \frac{1}{x_2^2}\left(\frac{1}{x_2-1} + \frac{x_2^3}{(x_2-1)(x_2'-1)} + \frac{1+x_2}{x_2'} - \frac{x_2^2}{x_2+x_2'-1}\right)\end{aligned} \tag{15}$$

where $b = \frac{dx_2'}{dx_2}$. To show τ is non constant near the complete structure, it is enough to show that $\frac{d\tau}{dx_2} \neq 0$ at the complete structure. First, we identify the complete structure.

Lemma 3.4. *The edge invariants for the complete structure are* $x_2 = x_2' = \frac{1}{6}(3+\sqrt{3}i)$, $y_2 = y_2' = \frac{1}{2}(-1+\sqrt{3}i)$ *and* $z_2 = z_2' = \frac{1}{2}(3+\sqrt{3}i)$.

Proof. In the complete structure, we have $H'(m_1) = H'(m_2) = 1$. Comparing (10) and (12) we get, $z_2 = z_2'$. Lemma 3.3 then shows $x_2 = x_2'$. Let $x_2 = x_2' = x$ and $z_2 = z_2' = z$. Edge Equation (9) then becomes:

$$\frac{z^2}{x^2}\frac{(1-z)^4}{(2z-z^2)^4} = \frac{(1-z)^4}{x^2 z^2 (2-z)^4} = 1 \tag{16}$$

From edge equation (8) we get, $x^2 = (x-1)^2(1-z)^2$. So, we have

$$1 - \frac{1}{x} = \pm\frac{1}{1-z} \Rightarrow x = \frac{1-z}{2-z} \quad \textit{or} \quad x = \frac{z-1}{z}$$

Substituting x in (16) we obtain,

$$(2-z)^2 z^2 = (1-z)^2 \quad \text{or,} \tag{17}$$

$$(2-z)^4 = (1-z)^2 \tag{18}$$

Using Mathematica ([10]), we see all solutions of (17) are real and (18) has only complex solution lying in the upper half plane: $z = \frac{3+\sqrt{3}i}{2}$. So, this $z = z_2 = z_2'$ corresponds to the complete solution. For this z, we have $x_2 = x_2' = x = \frac{z-1}{z} = \frac{3+\sqrt{3}i}{6}$ and $y_2 = y_2' = \frac{(-1+\sqrt{3}i)}{2}$. □

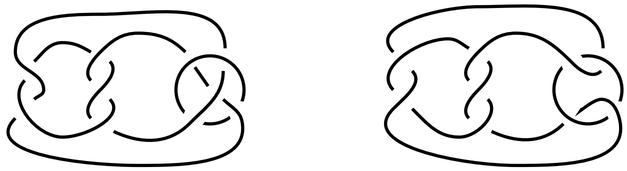

Figure 6. Two views of (the mirror image of) 9^2_{59}.

We use Lemma 3.3 to get,

$$x_2\left(1-\frac{1}{z_1'}\right)=x_2'\left(1-\frac{1}{z_1}\right)\Rightarrow x_2\left(1-\frac{z_1}{x_3x_3'}\right)=x_2'\left(1-\frac{1}{z_1}\right)$$

Differentiating both sides of the last equation with respect to x_2 gives us:

$$\left(1-\frac{z_1}{x_3x_3'}\right)-x_2\frac{d}{dx_2}\left(\frac{x_2'(x_3x_3'-1)^2}{x_3x_3'}\right)=b\left(1-\frac{1}{z_1}\right)+x_2'\left(\frac{1}{z_1^2}\frac{dz_1}{dx_2}\right)$$

$$\Rightarrow -\frac{x_2'}{(x_3x_3'-1)^2}x_3x_3'-x_2\frac{x_3x_3'\left(2(x_3x_3'-1)cx_2'+(x_3x_3'-1)^2b\right)-(x_3x_3'-1)^2x_2'c}{(x_3x_3')^2}$$

$$=b\left(1-\frac{1}{z_1}\right)+\frac{x_2'}{z_1^2}\left(c+2(x_3x_3'-1)cx_2'+(x_3x_3'-1)^2b\right),\text{ where}$$

$$c=\frac{d}{dx_2}(x_3x_3')=\frac{d}{dx_2}\left(\frac{(x_2-1)(x_2'-1)}{x_2x_2'}\right)=\left(1-\frac{1}{x_2}\right)\left(\frac{1}{x_2'}\right)^2b+\left(1-\frac{1}{x_2'}\right)\frac{1}{x_2^2}$$

We now use Mathematica ([10]) to solve for b at the complete structure (i.e. $x_2=x_2'=\frac{1}{6}(3+\sqrt{3}i)$) from the last equation to find $b=-1$. Plugging $b=-1$ and $x_2=x_2'=\frac{1}{6}(3+\sqrt{3}i)$ in (15), we again use [10] to get, $\frac{d\tau}{dx_2}=\frac{3}{2}(1-\sqrt{3}i)\neq 0$. This proves the proposition. $\square$

4. Other examples from the literature

Example 4.1. For any odd n, the $(-2,3,n)$ pretzel knot is obtained by $1/k$ surgery on the unknotted component of the link pictured on the left in Figure 6, where $k=(n-1)/2$. (Note that n must be odd for it to be a knot). This link is isotopic to the link on the right in the Figure, and by a further isotopy this link can be made into a mirror image of the link 9^2_{59} from Rolfsen's table. Hence its complement is isometric to that of 9^2_{59} (this can also be checked with SnapPy). So by Theorem 2.3, at most finitely many $(-2,3,n)$ pretzel knot complements have hidden symmetries.

In fact, Macasieb–Mattmann have shown that no hyperbolic $(-2,3,n)$ pretzel knot complements have hidden symmetries [13]. But we are not working as hard as they do, although our conclusion is weaker. And our methods apply equally well to, say, the $(2,3,n)$ pretzel knots, which are obtained from surgery on the unknotted component of a mirror image of 9^2_{57} (we leave this as an exercise for the reader).

Example 4.2. As Nathan Dunfield has pointed out to us, computations in his joint paper [1] with J.W. Aaber imply that at most finitely many knots obtained from the $(-2,3,8)$ pretzel link by $1/n$ surgery on its unknotted component can have complements with hidden symmetries, see Figure 2.6 there. This is despite the fact that each cusp of the complement has a square cross section (covering a $(2,4,4)$

triangle orbifold), since as recorded in [1] the $(-2,3,8)$ pretzel link complement is obtained by identifying faces of a single regular ideal octahedron.

The assertion instead follows from criterion (2) of Corollary 1.3, together with the proof of Theorem 5.5 of [1]. There the "Neumann–Zagier potential function" Φ on the deformation variety of the $(-2,3,8)$-pretzel link complement is shown to have a power series of the form

$$\Phi(\mathbf{u}) = c_1(u_1^2+u_2^2) + c_2(u_1^4+u_2^4) + c_3(u_1^2u_2^2) + O(|\mathbf{u}|^6),$$

where $c_1 = i$, $c_2 = (-3+i)/96$ and $c_3 = -(1+i)/16$. Here $\mathbf{u} = (u_1,u_2)$ is the complex length parameter from [19] that we also used in the proof of Theorem 1.2, and Φ is the potential function defined in Theorem 3 of [19] with the property that the longitude v_i of the ith cusp satisfies $v_i(\mathbf{u}) = \frac{1}{2}\partial\Phi/\partial u_i$ for each i. Since $\tau_i = v_i/u_i$ we have in this case that

$$\tau_1(\mathbf{u}) = c_1 + 2c_2u_1^2 + c_3u_2^2 + \dots$$

This is non-constant on the locus $u_1 = 0$ of hyperbolic structures where the first cusp is complete, since $c_3 \neq 0$. Since Φ is symmetric in u_1 and u_2 (reflecting the fact that the link complement has an involution exchanging the two cusps), τ_2 is also non-constant on the $u_2 = 0$ locus. Our conclusion therefore follows from Corollary 1.3(2) as claimed.

Example 4.3. Proposition 3.8 of [21] gives a criterion for showing that the complement of a fully augmented link in S^3 decomposes into regular ideal octahedra. For any such link L, Lemma 6.1 of [4] shows that $\pi_1(S^3 - L)$ is a subgroup of $\Gamma \rtimes \mathrm{Sym}(\mathcal{P})$, where $\mathcal{P}$ is the regular ideal octahedron, $\mathrm{Sym}(\mathcal{P})$ is its symmetry group, and Γ is the reflection group in its sides.

$\Gamma \rtimes \mathrm{Sym}(\mathcal{P})$ is generated by reflections in the sides of a fundamental domain for $\mathrm{Sym}(\mathcal{P})$. Such a fundamental domain has a single ideal point, and its cusp cross-section is a $(2,4,4)$-Euclidean triangle. It follows that each cusp of $S^3 - L$ covers the $(2,4,4)$-triangle orbifold, and in particular each determines a covering transformation-invariant horoball packing of $\mathbb{H}^3$ with fourfold rotational symmetry. This is the property that fails to hold for the examples considered in [15, Prop. 7.5].

It is easy to construct fully augmented links whose complements satisfy the criterion of [21, Prop. 3.8]. The first three members of one such family are pictured in Figure 7. Also pictured are the nerves of the circle packings determined by planar faces of the canonical right-angled ideal polyhedral decompositions of the augmented link complements. Section 2.1 of [21] describes the canonical right-angled ideal polyhedral decomposition of a fully augmented link complement, and its associated circle packings. The *nerve* of a circle packing of S^2 is the graph with a vertex at the center of each circle and an edge joining each pair of centers of mutually tangent circles.

Each nerve in Figure 7 but the leftmost is obtained from the one to its left by *central subdivision* [21, Def. 3.7]: add a vertex to the center of the triangle containing the top clasp of the augmented link, then join each existing vertex of this triangle to the new one with an edge. Since the leftmost nerve is the complete graph on four vertices, all of these nerves satisfy the criterion of [21, Prop. 3.8].

For each of these it is possible to strategically add crossings to yield links with a single non-clasp component, without changing the decomposition of the complement — only the way in which certain triangular faces are identified, see [21, Fig. 3]. All of these links satisfy condition (1) of Theorem 1.2, so this is a reasonable family

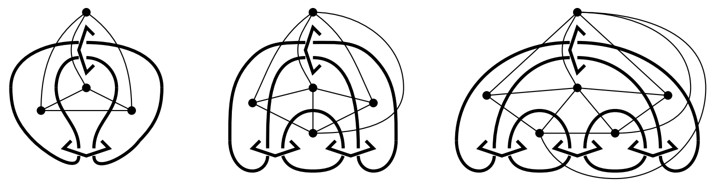

Figure 7.

to test techniques related to condition (2) for eliminating the possibility of "highly twisted" knot complements with hidden symmetries obtained by $1/n$-filling of their clasp components.

References

[1] John W. Aaber and Nathan Dunfield. Closed surface bundles of least volume. *Algebr. Geom. Topol.*, 10(4):2315–2342, 2010.

[2] Michel Boileau, Steven Boyer, Radu Cebanu, and Genevieve S. Walsh. Knot complements, hidden symmetries and reflection orbifolds. *Ann. Fac. Sci. Toulouse Math. (6)*, 24(5):1179–1201, 2015.

[3] Danny Calegari. Napoleon in isolation. *Proc. Amer. Math. Soc.*, 129(10):3109–3119 (electronic), 2001.

[4] Eric Chesebro, Jason DeBlois, and Henry Wilton. Some virtually special hyperbolic 3-manifold groups. *Comment. Math. Helv.*, 87(3):727–787, 2012.

[5] David Coulson, Oliver A. Goodman, Craig D. Hodgson, and Walter D. Neumann. Computing arithmetic invariants of 3-manifolds. *Experiment. Math.*, 9(1):127–152, 2000.

[6] Marc Culler, Nathan M. Dunfield, Matthias Goerner, and Jeffrey R. Weeks. SnapPy, a computer program for studying the geometry and topology of 3-manifolds. Available at http://snappy.computop.org (DD/MM/YYYY).

[7] The Sage Developers. *SageMath, the Sage Mathematics Software System (Version 7.5.1)*, 2017. http://www.sagemath.org.

[8] François Guéritaud. On canonical triangulations of once-punctured torus bundles and two-bridge link complements. *Geom. Topol.*, 10:1239–1284, 2006. With an appendix by David Futer.

[9] Neil R. Hoffman. On knot complements that decompose into regular ideal dodecahedra. *Geom. Dedicata*, 173:299–308, 2014.

[10] Wolfram Research, Inc. Mathematica, Version 11.1. Champaign, IL, 2017.

[11] Michael Kapovich. Eisenstein series and Dehn surgery. MSRI Preprint, 1992.

[12] Michael Kapovich. *Hyperbolic manifolds and discrete groups*, volume 183 of *Progress in Mathematics*. Birkhäuser Boston, Inc., Boston, MA, 2001.

[13] Melissa L. Macasieb and Thomas W. Mattman. Commensurability classes of $(-2, 3, n)$ pretzel knot complements. *Algebr. Geom. Topol.*, 8(3):1833–1853, 2008.

[14] Robert Meyerhoff. The cusped hyperbolic 3-orbifold of minimum volume. *Bull. Amer. Math. Soc. (N.S.)*, 13(2):154–156, 1985.

[15] Christian Millichap. Mutations and short geodesics in hyperbolic 3-manifolds. Preprint. arXiv:1406.6033, June 2014.

[16] Christian Millichap and William Worden. Hidden symmetries and commensurability of 2-bridge link complements. *Pacific J. Math.*, 285(2):453–484, 2016.

[17] Walter D. Neumann and Alan W. Reid. Arithmetic of hyperbolic manifolds. In *Topology '90 (Columbus, OH, 1990)*, volume 1 of *Ohio State Univ. Math. Res. Inst. Publ.*, pages 273–310. de Gruyter, Berlin, 1992.

[18] Walter D. Neumann and Alan W. Reid. Rigidity of cusps in deformations of hyperbolic 3-orbifolds. *Math. Ann.*, 295(2):223–237, 1993.

[19] Walter D. Neumann and Don Zagier. Volumes of hyperbolic three-manifolds. *Topology*, 24(3):307–332, 1985.

[20] Carlo Petronio and Joan Porti. Negatively oriented ideal triangulations and a proof of Thurston's hyperbolic Dehn filling theorem. *Expo. Math.*, 18(1):1–35, 2000.
[21] Jessica S. Purcell. An introduction to fully augmented links. In *Interactions between hyperbolic geometry, quantum topology and number theory*, volume 541 of *Contemp. Math.*, pages 205–220. Amer. Math. Soc., Providence, RI, 2011.
[22] John G. Ratcliffe. *Foundations of hyperbolic manifolds*, volume 149 of *Graduate Texts in Mathematics*. Springer, New York, second edition, 2006.
[23] Alan W. Reid and Genevieve S. Walsh. Commensurability classes of 2-bridge knot complements. *Algebr. Geom. Topol.*, 8(2):1031–1057, 2008.
[24] Dale Rolfsen. *Knots and links*, volume 7 of *Mathematics Lecture Series*. Publish or Perish, Inc., Houston, TX, 1990. Corrected reprint of the 1976 original.
[25] Makoto Sakuma and Jeffrey Weeks. Examples of canonical decompositions of hyperbolic link complements. *Japan. J. Math. (N.S.)*, 21(2):393–439, 1995.
[26] W. P. Thurston. The geometry and topology of 3-manifolds. mimeographed lecture notes, 1979.

Department of Mathematics, University of Pittsburgh
E-mail address: `jdeblois@pitt.edu`

Department of Mathematics, University of Pittsburgh
E-mail address: `prm50@pitt.edu`